ARTICLE

OBC
www.rsc.org/obc

Synthetic multifunctional pores: deletion and inversion of anion/cation selectivity using pM and pH

Naomi Sakai,[a] Nathalie Sordé,[a] Gopal Das,[a] Philippe Perrottet,[b] David Gerard[a] and Stefan Matile *[a]

[a] *Department of Organic Chemistry, University of Geneva, Geneva, Switzerland. E-mail: stefan.matile@chiorg.unige.ch; Fax: +41(0)22 328 7396; Tel: +41(0)22 702 6085*

[b] *Laboratoire de Spectrométrie de Masse, University of Geneva, Geneva, Switzerland*

Received 30th October 2002, Accepted 7th February 2003
First published as an Advance Article on the web 7th March 2003

We report the characterization of multifunctional rigid-rod β-barrel ion channels with either internal aspartates or arginine–histidine dyads by planar bilayer conductance experiments. Barrels with internal aspartates form cation selective, large, unstable and ohmic barrel-stave (rather than toroidal) pores; addition of magnesium cations nearly deletes cation selectivity and increases single-channel stability. Barrels with internal arginine–histidine dyads form cation selective ($P_{K^+}/P_{Cl^-} = 2.1$), small and ohmic ion channels with superb stability (single-channel lifetime > 20 seconds). Addition of "protons" results in inversion of anion/cation selectivity ($P_{Cl^-}/P_{K^+} = 3.8$); addition of an anionic guest (HPTS) results in the blockage of anion selective but not cation selective channels. These results suggest that specific, internal counterion immobilization, here magnesium (but not sodium or potassium) cations by internal aspartates and inorganic phosphates by internal arginines (but not histidines), provides access to synthetic multifunctional pores with attractive properties.

1 Introduction

Rigid-rod β-barrels[1,2] like **1** and **2**[3–7] are synthetic barrel-stave supramolecules developed to exploit the functional plasticity of their biological counterparts in bioorganic chemistry and beyond (Fig. 1). Their rare characteristics compared to the other synthetic ion channels/pores,[8–23] *i.e.* the possibility to install functional groups along the ion-conducting pathway, encouraged the shift of our interest from biomimicry to practical applications. Toward this end, *p*-octiphenyl β-barrel ion channels with internal histidine,[3,24–28] arginine,[3] lysine,[29–32] and aspartate residues[4–7] have been synthesized and used to recognize, translocate and, in some cases,[24–27] transform a broad variety of hydrophilic guests.

We have already reported the design and synthesis of rigid-rod β-barrel **1** with internal arginine–histidine (RH) dyads and β-barrel **2** with internal aspartates (D).[3–7] The formation of multifunctional pores has been demonstrated in spherical bilayer membranes, *i.e.*, EYPC SUVs or LUVs, for both cases. For instance, α-helix recognition by cationic supramolecule **1** in polarized vesicles confirmed the existence of multifunctional pores with internal RH dyads.[3] Barrel-stave (rather than toroidal)[5,33–35] type pores formed by the anionic supramolecule **2** in spherical bilayers[4] were shown to bind first Mg^{2+} and then various anionic substrates.[5] Thus, it was possible to monitor the enzymatic conversion of anionic compounds using inclusion complex **2** ⊃ $Mg^{2+}{}_n$.[6] Circular dichroism (CD) spectroscopy was used as a sensitive tool to elaborate on the structural basis of *p*-octiphenyl β-barrel pores including **2** under relevant conditions.[4,5,7] Ion channel characterization of barrels **1** and **2** in a planar bilayer has not been reported so far.

The introduction of arginines at the inner surface of rigid-rod β-barrels[1–7,24–32] was expected to yield ion channels with some of the characteristics of R-rich peptides in bilayer membranes.[36–47] This was of interest because pores formed by R-rich α-helical peptides, unlike lysine-rich peptide pores, exhibit concentration independent partition coefficients[36] and cation selectivity.[37–41] Moreover, R-rich α-L-peptides,[42,43] α-D-peptides,[42,43] β-L-peptides[44] and peptoids[45] derived from the HIV Tat translocation sequence[46,47] deliver hydrophilic organics to the cell nucleus as if the hydrophobic biomembrane barriers do not exist.[42–47]

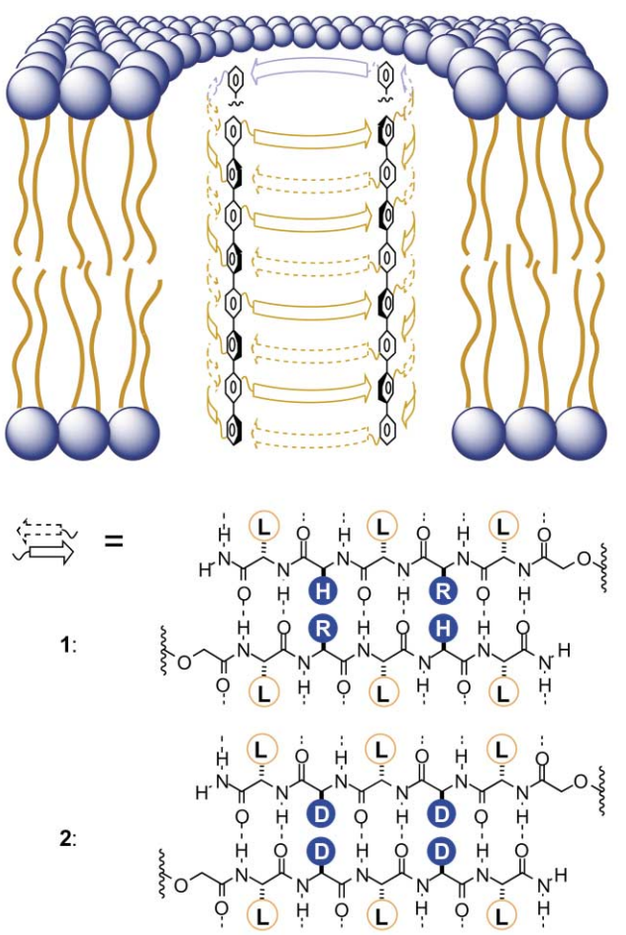

Fig. 1 Rigid-rod β-barrels **1** and **2** in lipid bilayers, depicted in blue (hydrophilic), gold (hydrophobic), and black (*p*-octiphenyl and β-sheet scaffolds); α-amino acid residues (one-letter abbreviations) located at the outer surface are black on white, internal ones white on blue. (Without X-ray structure data, the depicted suprastructures may be conceived as, at worst, productive working hypotheses that are consistent with *all* functions discovered so far.)

DOI: 10.1039/b210604c

Some, if not all, of the unique characteristics of R-rich peptides in bilayer membranes can be rationalized by tight binding of counteranions. For example, immobilization of dianions by guanidinium cations of R-rich peptides can provide the anionic surface expected within cation selective pores. Binding of univalent anions, on the other hand, can produce the hydrophobic zwitterions compatible with negligible contributions to bilayer surface charge[36] and unhindered phase transfer.[42–47] Eventual implications of the latter phenomenon on synthetic organic chemistry (*e.g.*, asymmetric phase transfer catalysis) have so far received little attention.[48] However, taking advantage of the favorable characteristics of guanidinium ions such as elevated pK_as, charge delocalization, and amplified ion pairing with carboxylates and phosphates due to bidentate hydrogen bonding, numerous synthetic guanidinium-rich hosts have been designed to recognize anionic guests.[49–56] Within this context, nano- to picomolar affinities for RNAs,[52] anionic α-helices,[3,53,54] inositol phosphates,[55] and AMP[56] have been reported for oligomeric alkylguanidinium cations.

Immobilization of inorganic phosphates by arginines (but not histidines)[7,24,25] within barrel **1** (or magnesium cations by aspartates within barrel **2**)[4–7] was therefore envisioned as a strategy to design synthetic multifunctional pores with controllable ion selectivity. Namely, protonation of internal histidines and arginine-bound phosphates was expected to result in conversion of anion-rich to cation-rich pores (Fig. 2). Similarly, binding of Mg^{2+} to the internal carboxylate anions should transform anion-rich to neutral and, eventually, to cation-rich pores. The electrostatics of the pore interior should then be reflected in their ion selectivity. So far, pH-gated inversion of anion/cation selectivity has been reported at elevated pH ≈ 9 for biological "α-barrel" pores with chemically introduced lysines[57] and pH-gated inversion of Ca^{2+}/Na^+ selectivity at pH ≈ 7 was demonstrated for poly-(*R*)-3-hydroxybutyrate ion channels with internal polyphosphates.[58] Here, we report the inversion of cation/anion selectivity at pH ≈ 5 of the stable and small, ohmic pores formed by barrel **1** and its usefulness to regulate molecular recognition within pores. The "unusual" nature of the RH-rich pores of **1** is highlighted by identification of the "usual" large and unstable, ohmic pores formed by D-rich barrel **2**, with cation selectivity that can be nearly nullified by binding of Mg^{2+}.

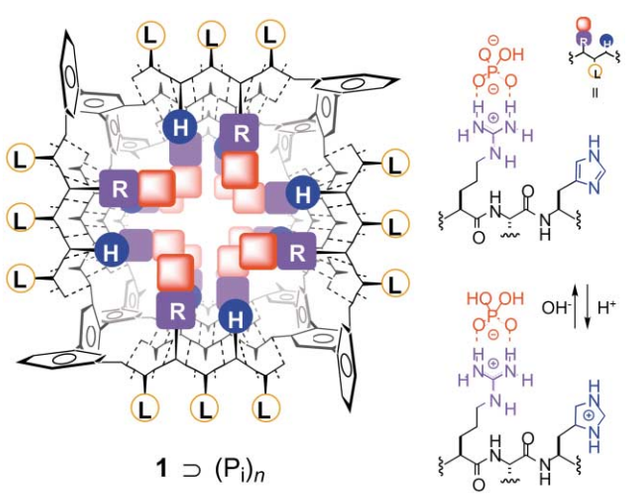

Fig. 2 Binding of inorganic phosphates within barrel **1** is expected to give **1** ⊃ $(P_i)_n$ with an anionic, small internal space at high pH and a cationic interior at low pH. Putative complex **1** ⊃ $(P_i)_n$ is shown at neutral pH as a simplified axial view in gold (hydrophobic residues), black (rigid-rod and β-sheet scaffolds), blue (basic residues), purple (cationic residues), and red (counteranions); β-strands are given as solid (backbone) and dotted lines (hydrogen bonds), see Fig. 1. The number *n* of internal phosphates and pK_as of internal guanidinium–phosphate complexes are unknown and the presence of counteranions other than P_i cannot be excluded.

2 Results and discussion

2.1 Multichannel characteristics of *p*-octiphenyl β-barrel 1

The activity of rigid-rod β-barrel **1** with internal arginine–histidine (RH) dyads in black (planar) lipid bilayers (BLMs) formed by egg yolk phosphatidylcholine (EYPC) was studied by conventional conductance experiments.[59] Conditions comparable to previous BLM-studies of H- and K-rich *p*-octiphenyl β-barrel ion channels were selected.[24,25,29–31] After the addition of barrel **1** (25 nM putative tetramer) at V = +50 mV, macroscopic ("multichannel") currents could be observed. Roughly ohmic I–V curves were consistent with formation of "dipole-free" β-sheets in the symmetric supramolecule **1**.

To elucidate anion/cation selectivity of pore **1**, a salt gradient between the *cis* (1 M KCl) and *trans* chambers (0.1 M KCl) was applied. Fig. 3 shows macroscopic I–V curves obtained under these asymmetric conditions at pH 6.0 (open) and pH 4.0 (closed). The reversal potential V_r exhibited sign inversion from negative at pH 6.0 to positive at pH 4.0. The permeability ratios calculated from V_r changed from P_{Cl^-}/P_{K^+} = 0.5 at pH 6.0 to P_{Cl^-}/P_{K^+} = 3.8 at pH 4.0. Inversion of anion/cation selectivity of channel **1** occurred at pH ≈ 5 (Fig. 4).

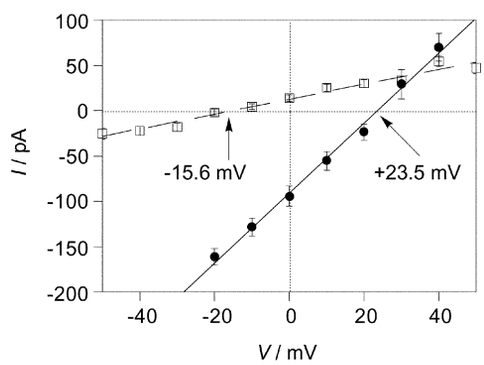

Fig. 3 Macroscopic I–V curve in asymmetric KCl (1.0 M *cis*, 0.1 M *trans*) for channel **1** (25 nM putative tetramer, *cis*) in EYPC BLMs at pH 4.0 (filled circles, 10 mM NaOAc) and pH 6.0 (open squares, 10 mM MES) with linear curve fit and reversal potentials.

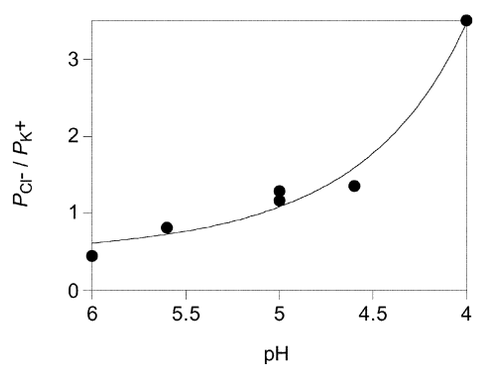

Fig. 4 Ion selectivity of channel **1** as a function of pH; data from macroscopic I–V curves as in Fig. 3 (10 mM NaOAc for 4.0 < pH < 5.6 and 10 mM MES for pH > 5.6) using GHK Eqn. (1).

High intrinsic pK_a ≈ 12.5 and reduced electrostatic interactions with delocalized charges of guanidinium cations suggested fully protonated arginine residues at pH = 6.0,[49–51] whereas nearly neutral histidines (intrinsic pK_a ≈ 6.0) can be assumed.[7] Cation selectivity of channel **1** with 32 putative internal RH dyads at pH = 6.0 therefore suggested the presence of at least some divalent counteranions. Electrospray ionization mass spectrometry suggested that inorganic phosphates P_i (*i.e.*, HPO_4^{2-}) play this role (Fig. 2). Fig. 5 shows a representative spectrum of the TFA salt of barrel **1** after denaturation with excess AcOH. Despite the presence of trifluoroacetic and acetic

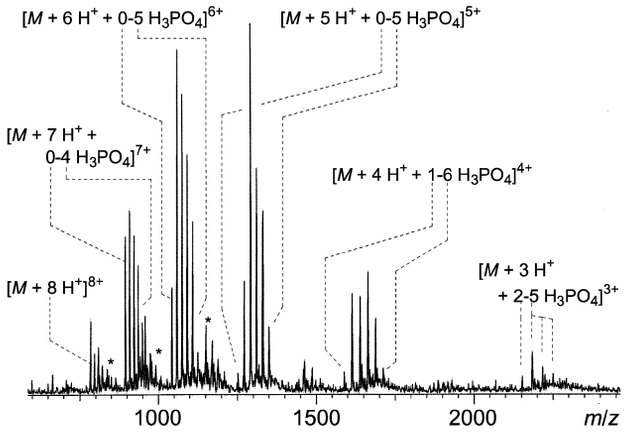

Fig. 5 Electrospray ionization mass spectra of disassembled barrel **1** under denaturising conditions (MeOH–MeCN–H_2O–AcOH = 50 : 37 : 12 : 1); (*): Low-intensity tails compatible with more complex counter-anion combinations.

acid, *p*-octiphenyls together with up to six inorganic phosphates *per* monomer were detected.

This finding was not surprising considering, for example, the binding of inorganic phosphates (K_D = 1.7 mM at V = +20 mV) rather than nitrates, sulfates, citrates, and perchlorates by bioengineered β-barrel pores with internal arginines,[55] or the nanomolar affinity of guanidinium-based amphiphiles for AMP at the air–water interface.[56] The precise number (n) of phosphates within the active ion channel **1** ⊃ $(P_i)_n$ remains, however, elusive, particularly since the presence of mixed complexes with additional counteranions can not be excluded. The pK_as of guanidinium–HPO_4^{2-} complexes within **1** ⊃ $(P_i)_n$ remain similarly obscure. However, reduction of a pK_a = 6.8 of HPO_4^{2-} with tetramethylammonium countercations in water to a pK_a = 4.8 in more hydrophobic environments has been reported.[51] It is thus reasonable to assume that neutralization of internal guanidinium–phosphate complexes together with protonation of internal imidazoles[7] contribute to conversion of cation to anion selectivity at pH ≈ 5.

2.2 Multichannel characteristics of *p*-octiphenyl β-barrel 2

Activity and ion selectivity of rigid-rod β-barrel **2** in *planar* bilayers were determined in a similar way using conditions that assured comparability with previous studies on Mg^{2+}-binding in *spherical* bilayers.[4–7] The most important difference from the conditions employed for **1** (and other rigid-rod β-barrels) was an approximately 10-fold decrease in ionic strength, and thus increased resistivity of the recording solution (see experimental section). Ohmic channels with a cation selectivity of P_{K^+}/P_{Cl^-} = 5.6 were found at pH = 6.0 (Fig. 6). High cation selectivity in *planar* bilayers was implicative of the presence of dissociable internal aspartates, and was consistent with previous results in *spherical* bilayers[5] and characteristics reported for biological "α-barrel" ion channels with chemically introduced internal glutamates.[60]

The presence of Mg^{2+} reduced the cation selectivity of channel **2** by 75% from P_{K^+}/P_{Cl^-} = 5.6 to P_{K^+}/P_{Cl^-} = 1.4. This almost negligible cation selectivity was consistent with our previous findings using *spherical* bilayers, showing permeability of metallopore **2** ⊃ $Mg^{2+}{}_n$ for anions as large as 5(6)-carboxyfluorescein and binding of various anionic guests to the internal $Mg^{2+}{}_n$–aspartate complexes.[5] The overall K_D ≈ 8.0 mM approximated for $Mg^{2+}{}_n$–aspartate complexes in *planar* bilayers was in good agreement with K_D = 2.9 mM and K_D = 5.3 mM found in *spherical* bilayers using two different assays.[4,5] The quantitative compatibility of the results on ion selectivity and Mg^{2+} binding obtained in planar and spherical bilayers must be highlighted.[32,61]

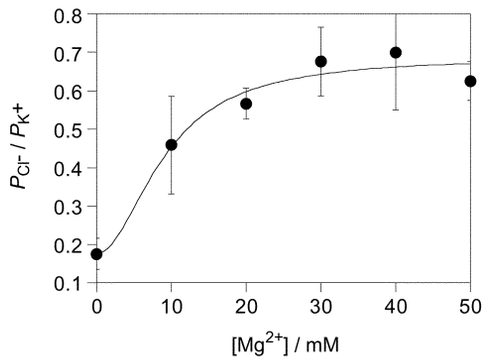

Fig. 6 Ion selectivity of channel **2** (20 nM tetramer *cis*) as a function of the concentration of $Mg(OAc)_2$; data from macroscopic *I–V* curves in a KCl gradient (0.1 M *cis*, 0.05 M *trans*) in EYPC BLMs at pH 6.0 (5 mM MES) using GHK Eqn. (1).

2.3 Single-channel characteristics of *p*-octiphenyl β-barrel 1

Single-channel characteristics of rigid-rod β-barrel **1** were determined under conditions nearly identical to those of the multichannel experiments described above. Lifetimes of seconds were observed for single anion channels at pH = 4.6 (Fig. 7a) as well as for single cation channels at pH = 6.0 (Fig. 7b). Higher stability of the single-channel conductance with mostly neutral histidines at pH = 6.0 compared to partially protonated histidines at pH = 4.6 was noted consistently and attributed to an increase in internal charge repulsion. The superb stability of single anion and particularly cation channels formed by $β_5$-barrel **1** was similar to that of contracted $β_3$-barrels, *i.e.*, barrels with β-sheets formed by tripeptides rather than pentapeptides.[25,30,31] The stability of channel **1** was, however, unprecedented for expanded *p*-octiphenyl $β_5$-barrels.[24]

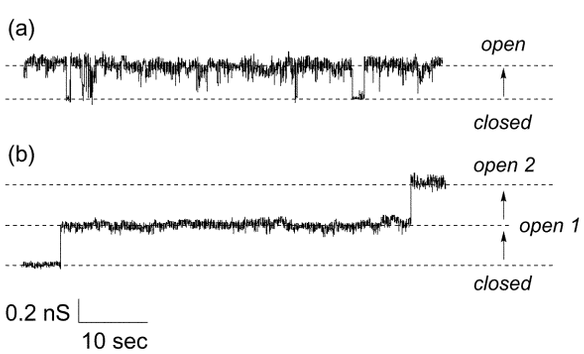

Fig. 7 Single-channel recordings for channel **1** in EYPC BLMs (1.0 M KCl, symmetric) at (a) pH 4.6 (10 mM NaOAc) and (b) pH 6.0 (10 mM MES); filtered at 20 Hz.

The single-channel conductance of barrel **1** showed little dependence on inversion of anion/cation selectivity at pH ≈ 5. According to the Hille model,[59,62,63] a single-channel conductance g = 0.3 nS corresponded to an inner diameter d ≈ 3.3 Å (Table 1). This value was in disagreement with the longer diameters expected from molecular models† [64] as well as internal recognition of more bulky α-helical peptides.[3] Moreover, the "short" diameter found with the $β_5$-barrel **1** contrasted sharply to the longer diameters determined for *p*-octiphenyl ion channels of similar $β_5$-barrel structures including **2** (d = 7–10 Å, see below).[24,25] The unusually small single-channel conductance was therefore, attributed to the presence of guanidinium–phosphate complexes within pore **1** (*i.e.*, **1** ⊃ $(P_i)_n$, Fig. 2). This

† According to molecular models, tetrameric supramolecules are the smallest self-assembly conceivable; trimeric barrels exhibit internal overcrowding around the *p*-octiphenyl turns and dimeric barrels with internal residues can not be constructed in molecular models.

Table 1 Summary of ion channel characteristics of barrels **1** and **2**

cds[a]	pH	Mg^{2+} [b]	P_{Cl^-}/P_{K^+} [c]	τ/ms [d]	*g*/nS [e]	*d*/Å [f]
1	6.0	−	0.48	>20000 [g]	0.30	3.3
1	4.6	−	3.75 [h]	20000	0.30	3.3
2	6.0	−	0.18	<0.5 [i]	0.26 [i]	10 [i]
2	6.0	+	0.70	12	0.26	8.8

[a] Compounds; see Fig. 1 for structures. [b] 0 (−) or 50 mM (+) $Mg(OAc)_2$. [c] Permeability ratio (calculated from GHK Eqn. (1)). [d] Mean single-channel lifetimes. [e] Single-channel conductances (from *I–V* curves using Ohm's law). [f] Inner channel diameter (from *g* using Hille's Eqn. (2)). [g] Approximated because of poor detectability of open/close transitions (see Fig. 7b). [h] pH = 4.0 (see Fig. 4). [i] Approximated because of poor detectability of single-channel conductances (see Fig. 8a).

interpretation was in agreement with cation selectivity at pH > 5.1 (Fig. 4) and multiple phosphates detected in the ESI MS (Fig. 5).

2.4 Single-channel characteristics of *p*-octiphenyl β-barrel 2

Single-channel characteristics of rigid-rod β-barrel **2** were determined under conditions comparable to those of the multichannel experiments described above as well as previous work in *spherical* bilayers.[4–7] Very short lifetimes $\tau < 0.5$ ms and ill-defined conductance levels ($g \approx 0.26$ nS) for open single channels were observed at pH = 6.0 (Fig. 8a).

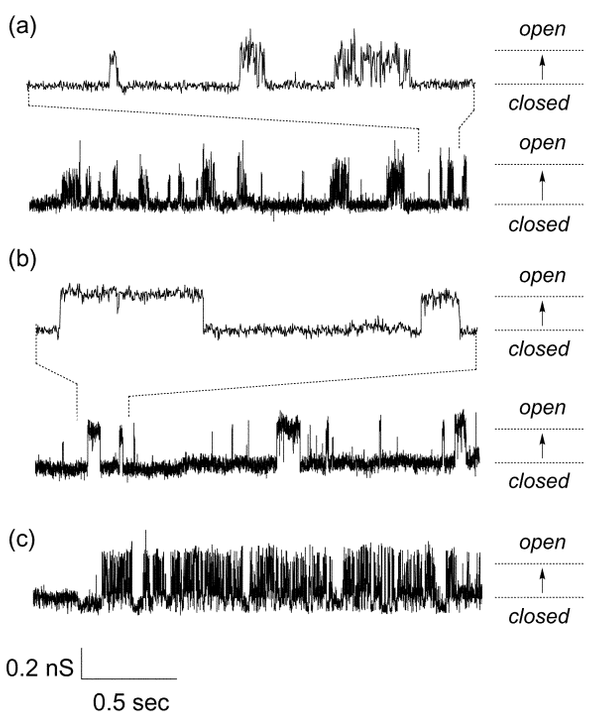

Fig. 8 Single-channel recordings for channel **2** in EYPC BLMs (0.1 M KCl, symmetric) at pH 6.0 (5 mM MES) in the absence (a) and presence of (b) 50 mM $Mg(OAc)_2$ and (c) 100 mM NaOAc; filtered at 1 kHz.

An average single-channel conductance of $g \approx 0.26$ nS corresponded, according to the Hille model,[59,62,63] to an inner diameter $d \approx 10$ Å for Mg^{2+}-free channel **2**. Considering the underestimates expected for small to medium sized pores,[25,62,63] $d \approx 10$ Å corresponded well with the inner diameters expected from molecular models[64] and previous results from *spherical* bilayers.[4–7] The inner diameter estimated for barrel **2** was 3-times (or 7 Å) longer than that of barrel **1** ⊃ $(P_i)_n$ (Table 1). In contrast to the stable, small channel **1** ⊃ $(P_i)_n$, the interior of Mg^{2+}-free channel **2** was thus not covered (and stabilized) by immobilized counterions.

The formation of internal Mg^{2+}–aspartate complexes increased the stability of barrel **2** more than 24-times (Fig. 8a *versus* b). Control experiments with Na^+ in place of Mg^{2+} corroborated that this single-channel stabilization indeed originated from specific Mg^{2+} binding, *i.e.* the formation of inclusion complex **2** ⊃ $Mg^{2+}{}_n$ (Fig. 8c). Different to guanidinium–phosphate ion pairs within barrel **1** ⊃ $(P_i)_n$, Mg^{2+}–carboxylate complexes within barrel **2** ⊃ $Mg^{2+}{}_n$ did not substantially reduce the single-channel conductance. This finding can be attributed to either the small size or some maintained mobility of internal magnesium cations.

Charge repulsion between dissociable internal carboxylates has been shown to result in pore destabilization and pore expansion using biological "α-barrels" with chemically introduced internal glutamates.[60] Similar conclusions were drawn from the pH profiles of barrel **2**[4,7] and synthetic "α-barrels" with internal glutamates[65–67] in spherical bilayers. The same explanation can be used to rationalize instability of cation selective channels formed by **2** (high charge repulsion) and stability of nearly non-selective ion channels **2** ⊃ $Mg^{2+}{}_n$ (low charge repulsion).

2.5 Molecular recognition within *p*-octiphenyl ion channel 1

The presence of internal immobilized phosphates suggested that molecular recognition of "large" organic anions within the "small" pore **1** ⊃ $(P_i)_n$ occurs by internal ion exchange. To verify this implication from spherical bilayers[3] in planar bilayer conductance experiments, multichannel dose response curves were recorded for 8-hydroxypyrene-1,3,6-trisulfonate (HPTS), a known blocker of *p*-octiphenyl β-barrels with internal histidines.[7,24,25] At pH = 4.6, increasing concentrations of HPTS (added *trans*) reduced the macroscopic current flowing through channel **1** (added *cis*) with an apparent $K_D \approx 30$ μM at $V = +50$ mV (Fig. 9, filled circles). Binding of anions within anion selective channel **1** ⊃ $(P_i)_n$ at pH = 4.6 was consistent with previous studies on *p*-octiphenyl β-barrels with internal histidines only.[24] Binding of "large" anions within "small" channel **1** ⊃ $(P_i)_n$ confirmed that internal anion exchange from **1** ⊃ $(P_i)_n$ to **1** ⊃ $(HPTS)_{n'}\cdot(P_i)_{n''}$ is possible. Preliminary results indicate that the esterolytic activity based on molecular recognition of 8-*R*-pyrene-1,3,6-trisulfonates within *p*-octiphenyl β-barrels[7,24–26] is maintained.[68]

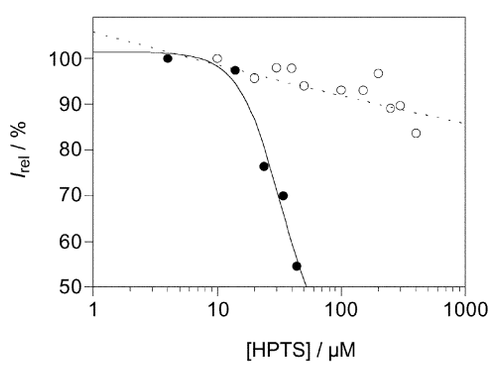

Fig. 9 Relative multichannel currents of channel **1** (80 nM tetramer *cis*) as a function of HPTS concentration in the *trans* chamber at pH = 4.6 (filled circles; 10 mM NaOAc, $I_{max} = 135$ pA) and pH = 6.0 (open circles; 10 mM MES, $I_{max} = 210$ pA) with $V = +50$ mV.

As expected from the ion selectivity, HPTS had little influence on the activity of channel **1** at pH = 6.0 (Fig. 9, open circles). Inversion from anion to cation selectivity of channel **1** ⊃ $(P_i)_n$ at pH ≈ 5, therefore, significantly lowered blockage activity of anion HPTS. This result suggested that *molecular recognition within multifunctional pores can be regulated by the selectivity of molecular translocation across the same pore*. However, it must be emphasized that alternative explanations

should never be excluded with such complex systems as the present one. Interestingly, HPTS blockage at pH = 5.0, *i.e.*, near selectivity inversion of channel **1** ⊃ $(P_i)_n$, was not detectable in a reproducible manner. We also failed to observe reproducible HPTS-binding at the single-channel level, presumably because of too small and/or too complex effects of internal ion exchange on the single-channel "signature".

3 Summary and conclusions

Rigid-rod β-barrels with internal arginine–histidine dyads form cation selective (P_{K^+}/P_{Cl^-} = 2.1), small ($d \approx 3.3$ Å), and stable (τ > 20 seconds) ion channels. Addition of "protons" results in inversion of anion/cation selectivity (P_{Cl^-}/P_{K^+} = 3.8) and the addition of an anionic guest results in partial blockage of anion ($K_D \approx 30$ μM), but not cation, selective channels. Barrels with internal aspartates form cation selective (P_{K^+}/P_{Cl^-} = 5.6), large ($d \approx 10$ Å), and unstable (τ < 0.5 ms) ion channels. Addition of magnesium cations ($K_D \approx 8$ mM) nearly demolishes cation selectivity (P_{K^+}/P_{Cl^-} = 1.4) and increases stability (τ = 12 ms).

Most findings for barrel-stave pores with internal aspartates corroborate previous trends with *p*-octiphenyl β-barrel ion channels that do not require further emphasis (*e.g.*, increase of channel diameter with β-sheet length, decrease of channel stability with β-sheet length, barrel stabilization by internal templates). Less obvious exceptions include the variable cation selectivity with Mg^{2+}. This effect was correctly predicted by studies in spherical bilayers[4,5] and could be understood as originating from immobilization of Mg^{2+}, a divalent countercation, but not univalent countercations such as K^+ by internal aspartates.

The complementary situation, that is, immobilization of inorganic phosphates, a divalent counteranion, by internal arginines but not histidines was predicted to create some of the less usual characteristics of rigid-rod β-barrels with internal arginine–histidine dyads. Seemingly counterintuitive phenomena like a polycationic synthetic pore exhibiting cation selectivity or a "small" ion channel host recognizing "large" anionic guests became accessible using specific counterion immobilization and ion exchange, respectively. The result is the first expanded *p*-octiphenyl β_5-barrel that forms stable ion channels (contracted *p*-octiphenyl β_3-barrel ion channels are "always" stable). This superb stability, coupled with the possibility of controlling molecular recognition and transformation[68] by inversion of cation/anion selectivity of molecular translocation, is promising for practical applications of multifunctional synthetic pores as sensors and catalysts.

4 Experimental section

4.1 Materials

EYPC was purchased from Northern Lipids Inc. (Vancouver, British Columbia, Canada), or from Avanti Polar Lipids (Alabaster, AL), HPTS from Molecular Probes (Eugene, OR), detergents, all salts and buffers of the best grade available from Sigma-Aldrich Corp (St. Louis, MO), and used as received. ESI-MS were recorded on a Finnigan MAT SSQ 7000.

4.2 $1^3,2^3,3^2,4^3,5^2,6^3,7^2,8^3$-Octakis(*Gla*-Leu-Arg-Leu-His-Leu-NH_2)-*p*-octiphenyl 1^m

Octiphenyl $\mathbf{1}^m$ was synthesized and purified as described in reference 3. Self-assembly of barrel **1** in spherical bilayers is described in reference 3. All indicated concentrations refer to a tetramer.

4.3 $1^3,2^3,3^2,4^3,5^2,6^3,7^2,8^3$-Octakis(*Gla*-Leu-Asp-Leu-Asp-Leu-NH_2)-*p*-octiphenyl 2^m

Octiphenyl $\mathbf{2}^m$ was synthesized, purified, and characterized as described in reference 4. Self-assembly of barrel **2** in spherical bilayers is described in references 4–7. All indicated concentrations refer to a tetramer.

4.4 BLM recordings

BLMs were formed by painting a solution of EYPC in *n*-decane (42 mg ml^{-1}) on an aperture (d = 150 μm, pretreated with the same solution) in a delrin cuvette separating two chambers containing 1 ml each of buffer and an agar bridge connection (1 M KCl) to Ag/AgCl electrodes (Warner Instrument Corp. Hamden, CT). Currents were recorded at different holding potentials (*trans* at ground) in a house-made Faraday cage, amplified (BC-525c, Warner Instrument Corp.), low-pass filtered with an 8-pole Bessel filter at 1–5 kHz (LPF-8, Warner Instrument Corp.), A–D converted (Digipack 1200–2, Axon Instruments, Union City, CA), and sampled at 10 kHz by computer (pClamp 8.0, Axon Instruments). If necessary, the data were further filtered using pClamp 8.0 or Origin (version 7, OriginLab). All the conductance measurements were performed at room temperature (22 ± 1 °C). Overall reliability of the employed system was regularly assessed using alamethicin. Conductances of multilevel channels and voltage dependence were fully reproducible and as in the literature.

Conditions for single- and multichannel experiments with identical *cis* and *trans* chambers for **1**: (a) 1.3 M KCl, 5 mM MES, pH = 5.0,[24] (b) 1.0 M KCl, 10 mM NaOAc, pH = 4.6, (c) 1.0 M KCl, 10 mM MES, pH = 6.0. Cation **1** (25 nM) was added to *cis* at V = +50 mV, anion HPTS (0–400 μM) was added to *trans* at V = +50 mV. Resistivity of the recording solution (a) was ρ = 7.716 Ωcm. Control experiments indicated decreasing probability of observing stable single channels with decreasing concentration of KCl and poor reproducibility of results around inversion of selectivity at pH 5.1.

Conditions for multichannel ion selectivity experiments with different *cis* and *trans* chambers for **1**: 1.0 M KCl in *cis*, 0.1 M KCl in *trans*, 10 mM NaOAc (pH < 5.6) or 10 mM MES (pH > 5.6) in both chambers.

Conditions for single- and multichannel experiments with identical *cis* and *trans* chambers for **2**: 0.1 M KCl, ± 50 mM $Mg(OAc)_2$,[4] ± 100 mM NaOAc, 5 mM MES, pH = 6.0. Tetramer **2** (20 nM) was added to *cis* at V = −50 mV. Besides the dominant g = 0.26 nS with 50 mM $Mg(OAc)_2$, a low conductance level g = 0.16 nS was occasionally observed. Resistivity of the recording solution with 50 mM $Mg(OAc)_2$ was ρ = 56.6 Ωcm. With 1.0 M KCl, the stabilization of single channels by Mg^{2+} was not observed. Conditions for multichannel ion selectivity experiments with different *cis* and *trans* chambers: 0.1 M KCl in *cis*, 0.05 M KCl in *trans*, 0–50 mM $Mg(OAc)_2$, 5 mM MES and pH = 6.0 in both chambers.

4.5 Data analysis

Permeability ratios were calculated from experimentally determined reversal potentials V_r (Fig. 3) using an equation derived from Goldman–Hodgkin–Katz (GHK) equation

$$P_{Cl^-}/P_{K^+} = [a_{K_c} - a_{K_t}\exp(-V_rF/RT)] / [a_{Cl_c}\exp(-V_rF/RT) - a_{Cl_t}] \quad (1)$$

where a_{K_c} and a_{K_t} are the activities of K^+ in the *cis* and *trans* chambers respectively, a_{Cl_c} and a_{Cl_t} the same for Cl^- [59] and plotted as a function of pH (Fig. 4) or Mg^{2+} concentration (Fig. 6).

Inner channel diameters d were approximated with Hille's model

$$1/g = l\,\rho/\pi\,(d/2)^2 + \rho/d \quad (2)$$

which assumes ion channels are electrolyte filled cylinders with ion channel conductance g (measured), ion channel length l (assumed as identical with length of the *p*-octiphenyl staves =

34 Å and the resistivity of the recording solution ρ (measured).[59,62] Note, as this model assumes unhindered movement of electrolyte within the pore, the estimated diameter is often smaller than reality.[63]

Dissociation constants were calculated using

$$\log (Y/(1 - Y)) = n\log[\text{guest}] - n\log K_D \qquad (3)$$

where Y is the fractional saturation $[(I^{max} - I) / (I^{max} - I^{min})]$, n the Hill coefficient, and K_D the dissociation constant.[5,59]

4.6 Abbreviations and symbols used

AMP, adenosine monophosphate; BLM, black (planar) lipid membrane; EYPC, egg yolk phosphatidylcholine; HPTS, 8-hydroxypyrene-1,3,6-trisulfonic acid, trisodium salt; LUV, large unilamellar vesicle; MES, 2-morpholinoethanesulfonic acid monohydrate; SUV, small unilamellar vesicle.

Acknowledgements

We thank Professor F. Gülaçar for assistance with ESI-MS and the Swiss NSF (2000–064818.01 and National Research Program "Supramolecular Functional Materials" 4047–057496) for financial support.

References

1 S. Matile, *Chem. Soc. Rev.*, 2001, **30**, 158–167.
2 S. Matile, *Chem. Rec.*, 2001, **1**, 162–172.
3 N. Sordé and S. Matile, *J. Supramol. Chem.*, in press.
4 G. Das and S. Matile, *Proc. Natl. Acad. Sci. U. S. A.*, 2002, **99**, 5183–5188.
5 G. Das, H. Onouchi, E. Yashima, N. Sakai and S. Matile, *ChemBioChem*, 2002, **3**, 1089–1096.
6 G. Das, P. Talukdar and S. Matile, *Science*, 2002, **298**, 1600–1602.
7 B. Baumeister, A. Som, G. Das, N. Sakai, F. Vilbois, D. Gerard, S. P. Shahi and S. Matile, *Helv. Chim. Acta*, 2002, **85**, 2740–2753.
8 P. Scrimin and P. Tecilla, *Curr. Opin. Chem. Biol.*, 1999, **3**, 730–735.
9 G. W. Gokel and A. Mukhopadhyay, *Chem. Soc. Rev.*, 2001, **30**, 274–286.
10 G. J. Kirkovits and C. D. Hall, *Adv. Supramol. Chem.*, 2000, **7**, 1–47.
11 V. Sidorov, F. W. Kotch, G. Abdrakhmanova, R. Mizani, J. C. Fettinger and J. T. Davis, *J. Am. Chem. Soc.*, 2002, **124**, 2267–2278.
12 P. Bandyopadhyay, P. Bandyopadhyay and S. L. Regen, *J. Am. Chem. Soc.*, 2002, **124**, 11254–11255.
13 L. M. Cameron, T. M. Fyles and C. W. Hu, *J. Org. Chem.*, 2002, **67**, 1548–1553.
14 A. J. Wright, S. E. Matthews, W. B. Fischer and P. D. Beer, *Chem. Eur. J.*, 2001, **7**, 3474–3481.
15 S. Das, D. Seebach and R. N. Reusch, *Biochemistry*, 2002, **41**, 5307–5312.
16 C. Goto, M. Yamamura, A. Satake and Y. Kobuke, *J. Am. Chem. Soc.*, 2001, **123**, 12152–12159.
17 H.-D. Arndt, A. Knoll and U. Koert, *Angew. Chem., Int. Ed.*, 2001, **40**, 2076–2078.
18 Y. R. Vandenburg, B. D. Smith, E. Biron and N. Voyer, *Chem. Commun.*, 2002, 1694–1695.
19 H. Carrasco, C. Foces-Foces, C. Perez, M. L. Rodriguez and J. D. Martin, *J. Am. Chem. Soc.*, 2001, **123**, 11970–11981.
20 L. Arnt and G. N. Tew, *J. Am. Chem. Soc.*, 2002, **124**, 7664–7665.
21 J. Sanchez-Quesada, M. P. Isler and M. R. Ghadiri, *J. Am. Chem. Soc.*, 2002, **124**, 10004–10005.
22 D. Wang, L. Guo, J. Zhang, L. R. Jones, Z. Chen, C. Pritchard and R. W. C. Roeske, *J. Pept. Res.*, 2001, **57**, 301–306.
23 J. M. Sanderson and S. Yazdani, *Chem. Commun.*, 2002, 1154–1155.
24 B. Baumeister, N. Sakai and S. Matile, *Org. Lett.*, 2001, **3**, 4229–4232.
25 A. Som, N. Sakai and S. Matile, *Bioorg. Med. Chem.*, 2003, **11**, 1363–1369.
26 A. Som and S. Matile, *Eur. J. Org. Chem.*, 2002, 3874–3883.
27 B. Baumeister and S. Matile, *Macromolecules*, 2002, **35**, 1549–1555.
28 G. Das, L. Ouali, M. Adrian, B. Baumeister, K. J. Wilkinson and S. Matile, *Angew. Chem., Int. Ed.*, 2001, **40**, 4657–4661.
29 N. Sakai and S. Matile, *J. Am. Chem. Soc.*, 2002, **124**, 1184–1185.
30 B. Baumeister, N. Sakai and S. Matile, *Angew. Chem., Int. Ed.*, 2000, **39**, 1955–1958.
31 N. Sakai, B. Baumeister and S. Matile, *ChemBioChem*, 2000, **1**, 123–125.
32 N. Sakai, D. Houdebert and S. Matile, *Chem. Eur. J.*, 2003, **9**, 223–232.
33 K. Matsuzaki, O. Murase, N. Fujii and K. Miyajima, *Biochemistry*, 1996, **35**, 11361–11368.
34 L. Yang, T. A. Harroun, T. M. Weiss, L. Ding and H. W. Huang, *Biophys. J.*, 2001, **81**, 1475–1485.
35 M. Zasloff, *Nature*, 2002, **415**, 389–395.
36 S. Stankowski, M. Pawlak, E. Kaisheva, C. H. Robert and G. Schwarz, *Biochim. Biophys. Acta*, 1991, **1069**, 77–86.
37 S. Lee, T. Tanaka, K. Anzai, Y. Kirino, H. Aoyagi and G. Sugihara, *Biochim. Biophys. Acta*, 1994, **1191**, 181–189.
38 T. Iwata, S. Lee, O. Oishi, H. Aoyagi, M. Ohno, K. Anzai, Y. Kirino and G. Sugihara, *J. Biol. Chem.*, 1994, **269**, 4928–4933.
39 Y. Agawa, S. Lee, S. Ono, H. Aoyagi, M. Ohno, T. Taniguchi, K. Anzai and Y. Kirino, *J. Biol. Chem.*, 1991, **266**, 20218–20222.
40 K. Anzai, M. Hamasuna, H. Kadono, S. Lee, H. Aoyagi and Y. Kirino, *Biochim. Biophys. Acta*, 1991, **1064**, 256–266.
41 U. Silphaduang and E. J. Noga, *Nature*, 2001, **414**, 268–269.
42 M. Green and P. M. Loewenstein, *Cell*, 1988, **55**, 2479–2494.
43 A. D. Frankel and C. O. Pabo, *Cell*, 1988, **55**, 1189–1193.
44 T. Suzuki, S. Futaki, M. Niwa, S. Tanaka, K. Ueda and Y. Sugiura, *J. Biol. Chem.*, 2002, **277**, 2437–2443.
45 S. Futaki, T. Suzuki, W. Ohashi, T. Yagami, S. Tanaka, K. Ueda and Y. Sugiura, *J. Biol. Chem.*, 2001, **276**, 5836–5840.
46 N. Umezawa, M. A. Gelman, M. C. Haigis, R. T. Raines and S. H. Gellman, *J. Am. Chem. Soc.*, 2002, **124**, 368–369.
47 P. A. Wender, D. J. Mitchell, K. Pattabiraman, E. T. Pelkey, L. Steinman and J. B. Rothbard, *Proc. Natl. Acad. Sci. U. S. A.*, 2000, **97**, 13003–13008.
48 T. Schlama, L. Alcaraz and C. Mioskowski, *Synlett*, 1996, 571–572.
49 F. P. Schmidtchen and M. Berger, *Chem. Rev.*, 1997, **97**, 1609–1646.
50 T. S. Snowden and E. V. Anslyn, *Curr. Opin. Chem. Biol.*, 1999, **3**, 740–746.
51 B. Dietrich, D. L. Fyles, T. M. Fyles and J.-M. Lehn, *Helv. Chim. Acta*, 1979, **62**, 2763–2787.
52 R. J. Austin, T. Xia, J. Ren, T. T. Takahashi and R. W. Roberts, *J. Am. Chem. Soc.*, 2002, **124**, 10966–10967.
53 M. W. Peczuh and A. D. Hamilton, *Chem. Rev.*, 2000, **100**, 2479–2494.
54 B. Orner, X. Salvatella, J. Sanchez Quesada, J. de Mendoza, E. Giralt and A. D. Hamilton, *Angew. Chem., Int. Ed.*, 2002, **41**, 117–119.
55 S. Cheley, L. Gu and H. Bayley, *Chem. Biol.*, 2002, **9**, 829–838.
56 K. Ariga and T. Kunitake, *Acc. Chem. Res.*, 1998, **31**, 371–378.
57 V. Borisenko, M. S. P. Sansom and G. A. Woolley, *Biophys. J.*, 2000, **78**, 1335–1348.
58 S. Das and R. N. Reusch, *Biochemistry*, 2001, **40**, 2075–2079.
59 B. Hille, *Ionic channels of excitable membranes*, 2nd Edn., Sinauer, Sunderland, MA, 1992.
60 K. Asami. T. Okazaki, Y. Nagai and Y. Nagaoka, *Biophys. J.*, 2002, **83**, 219–228.
61 G. Menestrina, K.-P. Voges, G. Jung and G. Boheim, *J. Membr. Biol.*, 1986, **93**, 111–132.
62 C. C. Cruickshank, R. F. Minchin, A. C. Le Dain and B. Martinac, *Biophys. J.*, 1997, **73**, 1925–1931.
63 O. S. Smart, J. Breed, G. R. Smith and M. S. P. Sansom, *Biophys. J.*, 1997, **73**, 1109–1126.
64 B. Baumeister and S. Matile, *Chem. Eur. J.*, 2000, **6**, 1739–1749.
65 N. K. Subbarao, R. A. Parente, F. C. Szoka Jr, L. Nadasdi and K. Pongracz, *Biochemistry*, 1987, **26**, 2964–2972.
66 R. A. Parente, S. Nir and F. C. Szoka Jr, *Biochemistry*, 1990, **29**, 8720–8728.
67 F. Nicol, S. Nir and F. C. Szoka Jr, *Biophys. J.*, 2000, **78**, 818–829.
68 N. Sakai and S. Matile, unpublished results.